## ORIGINAL RESEARCH

Protective Role of microRNA-31 in Acetaminophen-Induced Liver Injury: A Negative Regulator of c-Jun N-Terminal Kinase (JNK) Signaling Pathway

Jianxin Zheng,[1,5,*] Hong Zhou,[2,*] Taihua Yang,[1] Jinchuan Liu,[1] Tian Qin,[1] Xiangqian Gu,[1] Ji Wu,[1] Yi Zhang,[6] Honglin Wang,[2] Yuanjia Tang,[3] Feng Xue,[1] Yimin Mao,[4] and Qiang Xia[1]

[1]Department of Liver Surgery and Liver Transplantation Center, Renji Hospital, Shanghai Jiaotong University School of Medicine, Shanghai, China; [2]Center for Microbiota and Immunological Diseases, Shanghai General Hospital, Shanghai Institute of Immunology, Shanghai Jiaotong University School of Medicine, Shanghai, China; [3]Shanghai Institute of Rheumatology, Renji Hospital, Shanghai Jiaotong University School of Medicine, Shanghai, China; [4]Division of Gastroenterology and Hepatology, Shanghai Institute of Digestive Disease, Shanghai Jiaotong University School of Medicine, Shanghai, China; [5]Department of Urology, Xiamen Branch, Zhongshan Hospital, Fudan University, Xiamen, China; and [6]ABLife Institute of BioBigData, East Lake High-Tech Development Zone, Wuhan, China
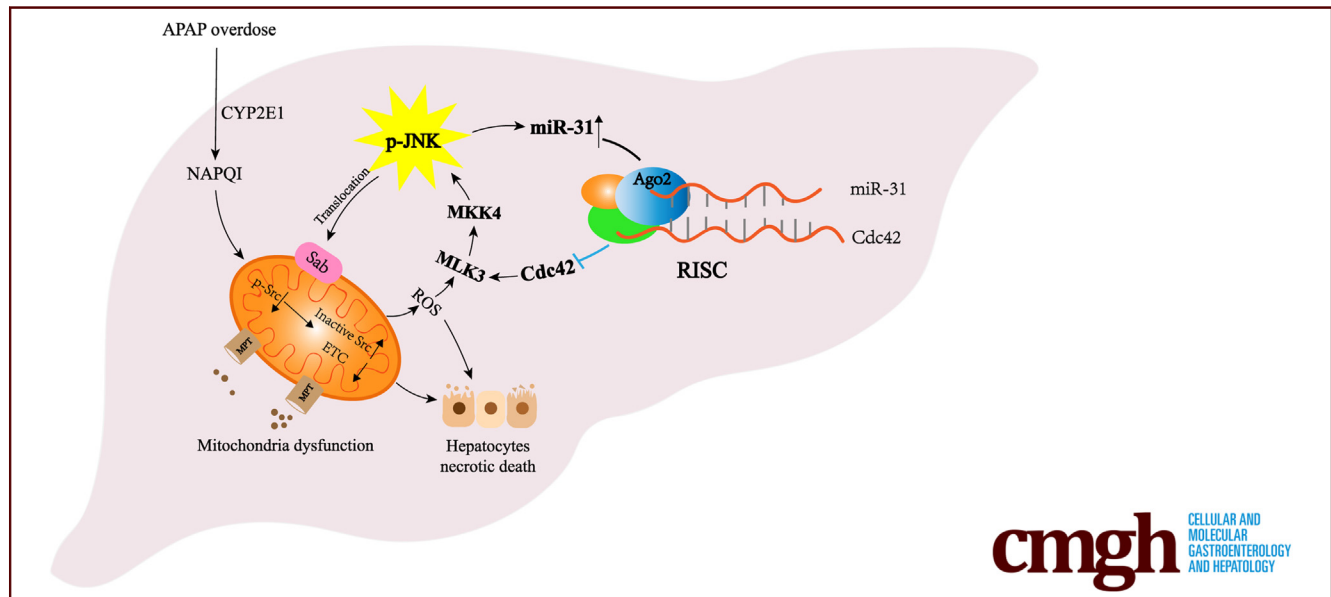
SUMMARY

The post-transcriptional regulator microRNA-31 plays a protective role in acetaminophen-induced liver injury. Indeed, although acetaminophen overdose leads to c-Jun N-terminal kinase (JNK) signaling overactivation, there is a safety mode, the feedback loop of JNK/microRNA-31/Cdc42, induced by JNK signaling itself, to maintain hepatocyte homeostasis.

BACKGROUND & AIMS: Sustained c-Jun N-terminal kinase (JNK) activation plays a major role in drug-induced liver injury (DILI). Stress-responsive microRNA-31 (miR-31) has been implicated in regulating different cellular damage, and JNK activation could induce miR-31 expression. However, the regulatory role of miR-31 in DILI has not been studied previously.

We aimed to investigate whether miR-31 could ameliorate DILI and ascertain potential molecular mechanism.

METHODS: miR-31 gene knockout (31-KO) and wild-type *C57BL/6J* mice were used to construct an acetaminophen (APAP)-induced DILI model. Primary mouse hepatocytes, as well as alpha mouse liver 12 (AML-12) cell lines, were used for in vitro experiments. Argonaute 2–associated RNA immunoprecipitation combined with high-throughput sequencing were performed to identify specific targets of miR-31.

RESULTS: 31-KO mice showed a higher mortality rate, liver transaminase levels, and hepatic necrosis compared with those in wild-type mice after APAP-induced hepatotoxicity. The protective role of miR-31 on hepatocytes has been analyzed via constructing bone marrow chimeric mice. Mechanistically, we found that hepatic JNK phosphorylation increased significantly in 31-KO mice. This caused mitochondrial phosphorylated Src (p-Src) inactivation and more reactive oxygen species produc-

tion, which directly amplifies hepatocyte necrotic cell death, while administration of JNK-specific inhibitor SP600125 could abrogate the differences. Moreover, bioinformatics analysis of RNA immunoprecipitation combined with high-throughput sequencing identified that guanosine triphosphatase, cell division cycle protein 42 (Cdc42), the upstream molecule of JNK signaling, was the specific target of miR-31 and could form a miR-31/Cdc42/phosphorylated mixed-lineage kinase 3 (p-MLK3) negative feedback loop to restrict JNK overactivation. Clinically, both miR-31 and phosphorylated JNK (p-JNK) were highly increased in liver tissues of DILI patients with different etiologies.

CONCLUSIONS: miR-31 can down-regulate Cdc42 to restrict overactivation of reactive oxygen species/JNK/mitochondria necrotic death loop in hepatocytes of APAP-induced DILI, which might provide a new therapeutic target for alleviating JNK overactivation–based liver injury. *(Cell Mol Gastroenterol Hepatol 2021;12:1789–1807; https://doi.org/10.1016/j.jcmgh.2021.07.011)*

Drug-induced liver injury (DILI) is a common cause of severe liver disease caused by medication exposure. A majority of DILI occurs as a result of either accidental or intentional overdose intake of acetaminophen (APAP), which is one of the most widely used analgesic and antipyretic drug in developed countries. APAP is safe at therapeutic doses, but its overdose can cause hepatotoxicity and even acute liver failure.[1] However, the diagnosis and treatment of DILI are challenging for clinicians because of its insidious onset, fast progress, and lack of specific biomarkers. A DILI diagnosis often relies on subjective addition of clinical, biochemical, and histologic information. Clinically, N-acetyl cysteine is the only therapeutic option for an APAP-overdose DILI, but this mediation has some limitations, including a narrow therapeutic window and adverse effects.[2] Hence, new effective measurements and studies on the mechanisms of DILI are urgently needed.

APAP-induced DILI is the most common intrinsic DILI, and a lot of effort has been made to uncover its hepatotoxicity mechanisms. Oxidative stress–induced c-Jun N-terminal kinase (JNK) overactivation and mitochondrial dysfunction are considered to be the predominant cellular events in APAP-induced necrotic cell death.[3] APAP is taken up from the intestine within a few hours after consumption. The majority of APAP is metabolized in the liver via glucuronidation (50%–60%) and sulfation (25%–30%). A small fraction of APAP (10%–15%) is metabolized by cytochrome P450 isoforms 2E1[4] into a powerful electrophilic intermediate N-acetyl-p-benzoquinone imine, which can be converted by glutathione (GSH) into a harmless reduced form. However, when GSH is depleted owing to APAP overdose, enhanced generation of reactive oxygen species (ROS) are contributing to the activation of mitogen-activated protein kinase cascade, leading to phosphorylation of c-Jun N-terminal kinase (p-JNK). Then, translocation of p-JNK to the C terminus of SH3 homology associated BTK

binding protein (Sab) on the outside of mitochondria leads to docking protein 4–dependent dephosphorylation of active phosphorylated Src (p-Src) on the inner membrane.[5] The inactivation of intramitochondrial Src inhibits electron transport and adenosine triphosphate synthesis, then promotes ROS production, which sustains JNK activation and causes the opening of the mitochondrial membrane permeability pore. The permeabilization and lysis of the mitochondrial membrane lead to the release of endonuclease G and apoptosis-inducing factor, which subsequently translocate to nuclei causing nuclear DNA fragmentation.[6] These processes finally result in centrilobular necrotic cell death and liver injury.[5,7] Besides intrinsic DILI, both activation of JNK signaling pathway and mitochondrial dysfunction are also indispensable events involving in the pathophysiology of idiosyncratic DILI, a rare but serious liver disease caused by quite a few drugs in a small subset of patients.[8]

In the past decade, microRNAs (miRNAs) have represented a broad class of 18–22 nucleotide noncoding RNAs that negatively regulate gene expression at the post-transcriptional level. miRNA temporal and spatial heterogeneity expressions are exerting a critical role in various biological processes. Previous studies on miRNAs in DILI are mostly limited to circulating biomarkers.[9] However, there are a few studies exploring the specific mechanism by which miRNAs regulate DILI.[10,11] In our previous studies, we showed that up-regulation of microRNA-31 (miR-31) could enhance keratinocyte proliferation on the epidermis in psoriasis,[12] or negatively regulate peripherally derived regulatory T-cell generation in autoimmune disease.[13] However, emerging evidence has indicated that miR-31 is also a stress-responsive miRNA, which plays an important role in the regulation of different damaged cells. Tian et al[14] have shown that, in response to ionizing radiation injury, an increased level of miR-31 in intestinal stem cells could support cell survival and activate their repair mechanisms. In oxidative stress–induced neuronal injury, up-regulated miR-31 alleviates neuron injury by down-regulating the Janus kinase/signal transducer and activator of transcription 3 pathway, reducing inflammatory response.[15] It also has been suggested that miR-31 serves as an important cell-

Most current article

autonomous mediator by activating the RAS/mitogen-activated protein kinase (MAPK) signaling pathway, promoting wound healing in skin injury.[16] Furthermore, previous research has shown that JNK activation could induce miR-31 expression in colon cancer cells,[17] and activation of JNK signaling is a critical event in APAP-induced DILI,[18,19] However, whether miR-31 actually plays a functional role in DILI, and what that role may be, remains to be elucidated.

The aim of the current study was to identify the regulatory role and specific mechanism of miR-31 in APAP-induced DILI. We show that deletion of miR-31 exacerbates JNK signaling, inducing mitochondrial dysfunction and necrotic cell death after APAP injection. Up-regulation of miR-31 induced by JNK activation could suppress small guanosine triphosphatase Cdc42, limiting JNK signaling overactivation and, subsequently, protecting against liver injury.

Results

miR-31 Knockout Mice Developed More Severe Liver Injury Than WT Mice

To identify the potential role of miR-31 on APAP-induced DILI, miR-31 WT and knockout mice (31-KO) were injected intraperitoneally with a nonlethal dose of APAP (300 mg/kg), and mortality rate was monitored for 4 days. During the whole observation period, the survival rate in APAP-treated 31-KO mice was much lower than that observed in WT mice (Figure 1A). Notably, the APAP-induced increase of serum levels of both alanine aminotransferase (ALT) and aspartate aminotransferase (AST), 2 classic serum markers of liver injury, was greater in 31-KO mice than that observed in WT mice at 24 hours after APAP injection (Figure 1B). However, at 6 hours, there was only a difference in serum ALT level between KO and WT mice, indicating early change of liver injury among them. The extent of liver necrosis (Figure 1C) and histopathologic analysis (Figure 1D) of necrosis also was much more severe in 31-KO mice than that observed in WT controls at both 6 and 24 hours after APAP injection. Consistent with histopathology, DNA fragmentation, a characteristic feature of APAP-induced necrotic cell death, was increased substantially in livers of APAP-treated 31-KO mice (Figure 1E).

In addition, an innate inflammation infiltration including neutrophil, monocyte, and Kupffer cells was detected in the liver tissue by flow cytometric analysis (Figure 2A), showing that the proportion of infiltrating neutrophils in 31-KO mice was significantly higher than that of WT mice at both 6 (Figure 2B) and 24 hours (Figure 2C) after APAP injection. The miR-31 deficiency enhanced APAP-evoked liver damage.

miR-31 Expression Was Increased in Both Hepatocytes and Nonparenchymal Cells and Confined Mainly to the Hepatic Pericentral Vein Area in APAP-Induced DILI

To gain further insight into the miR-31 expression profile, we examined the time course of miR-31 expression in hepatocytes and nonparenchymal cells (NPCs) isolated from APAP-challenged mice. The purity of isolated hepatocytes and NPCs was confirmed with specific markers by flow cytometry or immunofluorescence. Our results showed that hepatocyte purity was very high, and NPCs were basically free of hepatocytes and composed mainly of immune cells (Figure 3A and B).

We found that miR-31 expression increased to peak in approximately 3 hours, then decreased to nearly normal levels at the next several time points in hepatocytes (Figure 3C). In hepatic NPCs, the expression of miR-31 also increased dynamically, and the peak appeared at 3 hours (Figure 3C). To determine the histologic enhanced miR-31 expression region, we also performed the time course experiments of in situ miRNA hybridization on liver cryosections. We found that miR-31 expression during the injured period was confined mainly to the hepatic pericentral vein area (Figure 3D), which was more vulnerable to APAP hepatotoxicity, containing damaged hepatocytes and infiltrating inflammatory cells. In contrast, histologic miR-31 expression decreased to nearly normal levels at 72 hours, the time mostly recovered from liver injury. Thus, the findings indicated that miR-31 was increased in both hepatocytes and NPCs, and may play important roles in APAP-induced DILI.

miR-31 Exerted a Protective Role Mainly Through Hepatocytes in DILI

Infiltrating inflammatory cells have been implicated in engaging in APAP-induced liver damage, and our previous study has shown that miR-31 could negatively regulate peripherally derived regulatory T-cell generation in autoimmune inflammatory diseases.[13] To decipher whether miR-31 plays the protective role via hematopoietic-derived inflammatory cells, we also generated reciprocal bone marrow chimeric mice (Figure 4A). After being lethally irradiated to clean out host bone marrow, WT or 31-KO mice then were injected with 31-KO or WT bone marrow, respectively, to generate the chimeric mice with specific deletion of miR-31 in a hematopoietic-derived immune system (KO BM-WT) or non–hematopoietic-derived resident cells (WT BM-KO). A normal control group (WT BM-WT) also was set. Unexpectedly, the mortality rate of the WT BM-KO group was higher than in the other 2 groups (Figure 4B), and it also showed a marked increase both in serum ALT and AST levels compared with the KO BM-WT and WT BM-WT groups after 24 hours of APAP administration (Figure 4C). The histopathology results (Figure 4D) and histologic necrosis evaluation (Figure 4E) were consistent with the levels of serum marker. Thus, combined with results in Figure 3C and D, the chimeric mice experiment precludes the protective role of miR-31 in infiltrating inflammatory cells, and suggests that miR-31 exerts a protective role mostly through hepatocytes in APAP-induced DILI. To further confirm the role of miR-31 in hepatocytes, mouse primary hepatocytes were transfected with miR-31 mimic or inhibitor, and then incubated with APAP for 6 hours. As expected, miR-31 overexpression significantly
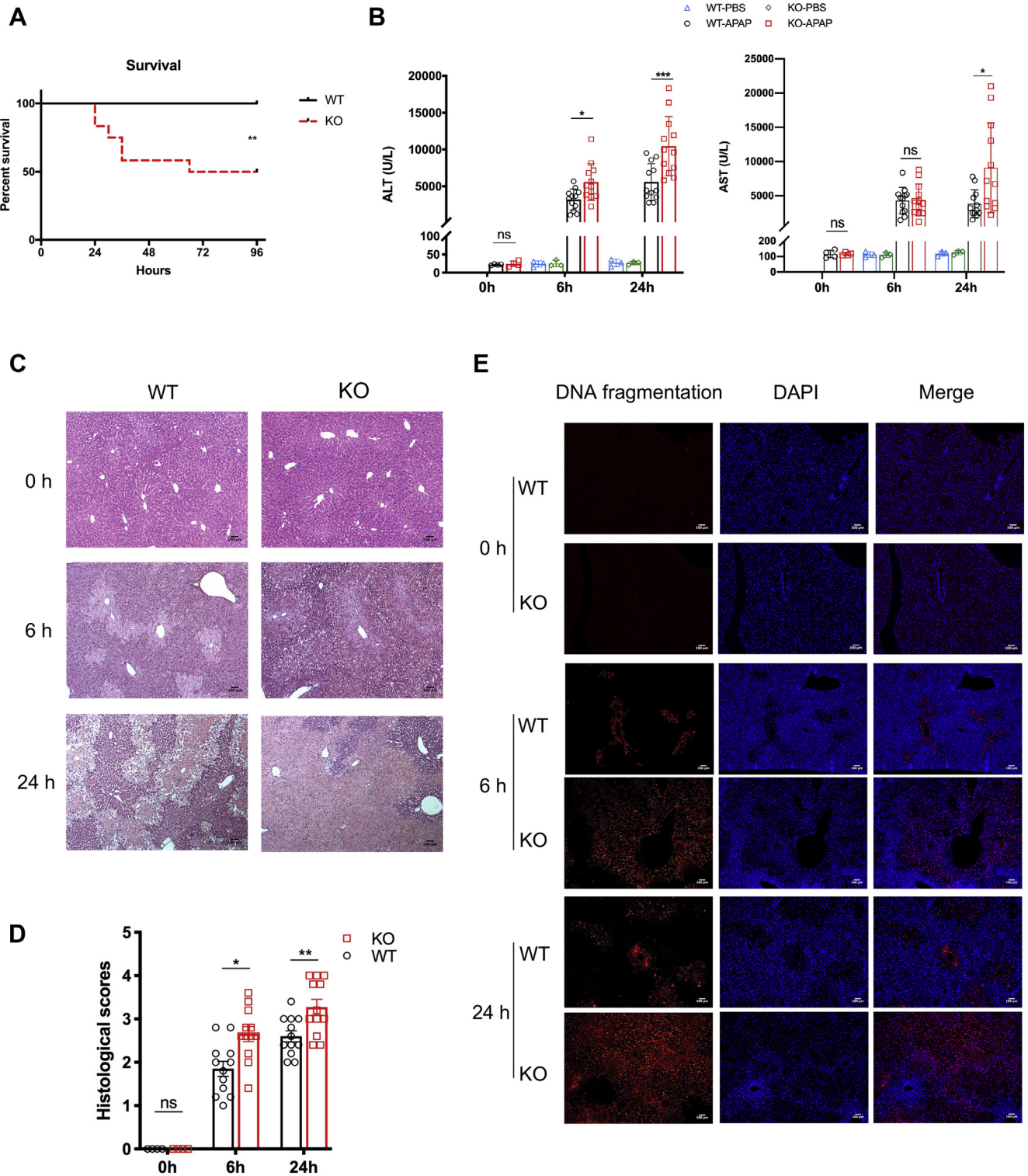
Figure 1. miR-31 KO mice developed more severe liver injury than WT mice. (*A*) Survival rate of 31-KO and WT mice after APAP administration. n = 12 mice per group. (*B*) The level of serum ALT and AST in 31-KO and WT mice after APAP challenge, and respective vehicle (phosphate-buffered saline [PBS]) controls also were set. n = 3–12 mice per group. (*C and D*) H&E staining of (*C*) injured liver tissue and (*D*) necrotic histopathologic evaluation in 31-KO and WT mice at 0, 6, and 24 hours after APAP injection. n = 4–12 mice per group. (*E*) Terminal deoxynucleotidyl transferase–mediated deoxyuridine triphosphate nick-end labeling staining (for DNA fragmentation) in the liver section of 31-KO and WT mice at 0, 6, and 24 hours after APAP injection. Red indicates DNA fragmentation, blue indicates 4′,6-diamidino-2-phenylindole (DAPI) staining. Data are representative of means ± SD. *$P < .05$; **$P < .01$, and ***$P < .001$, 2-tailed Student t test.
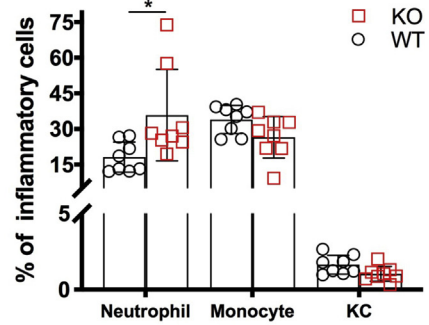
A
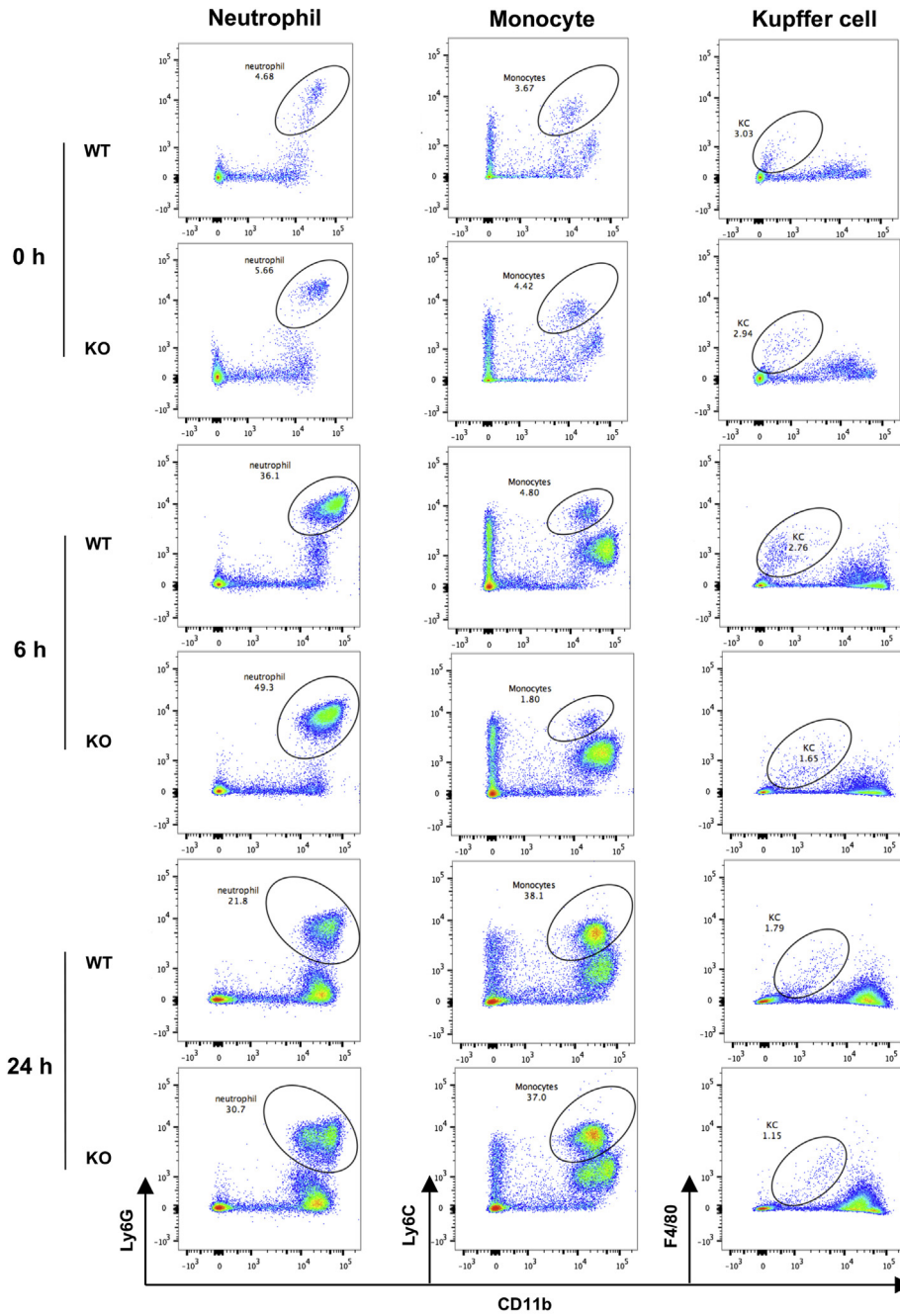
B
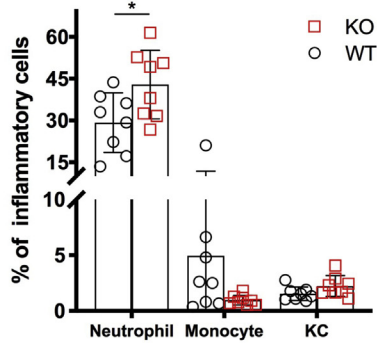
C

attenuated hepatocyte necrosis, and miR-31 inhibition aggravated hepatocyte necrosis, compared with normal control (Figure 4F).

miR-31 Alleviated DILI Mainly via the JNK Signaling Pathway

To preclude the possibility that aggravated APAP-induced liver injury in 31-KO mice was caused by altered APAP metabolism, we examined the expression of APAP metabolic enzyme and the time course of GSH consumption. No differences in cytochrome P450 isoforms 2E1 and cytochrome P450 isoforms 1A2 expression were observed in basal or post-APAP injection between 31-KO and WT mice (Figure 5A). Levels of hepatic basal GSH or GSH depletion at 3 or 6 hours after APAP injection also were not altered significantly between 31-KO and WT mice (Figure 5B).

To further decipher the mechanism by which miR-31 ameliorates APAP hepatotoxicity, liver tissues collected from 31-KO and WT mice 6 hours after APAP injection were subjected to high-throughput RNA sequencing and differentially expressed genes (DEGs) were analyzed by Kyoto Encyclopedia Genes and Genomes pathway enrichment. DEGs between 31-KO and WT from the top 10 pathways (total, 46 genes; 33 genes were up-regulated, 13 genes were down-regulated) are shown in Figure 5C. The pathway enrichment results have suggested that the MAPK signaling pathway, phosphatidylinositol 3-kinase (PI3K)-protein kinase B (Akt) signaling pathway, peroxisome proliferator activated receptor (PPAR) signaling pathway, and retinol metabolism might have been involved in the differential manifestation between 31-KO and WT mice after APAP injection (Figure 5D). The JNK signaling pathway was one of the major subfamilies of the MAPK pathway,[20] and the genes enriched in the MAPK pathway also were closely related to JNK signaling. As indicated in previous studies, the JNK signaling pathway plays a critical role in hepatocytes of APAP-induced DILI.[18,19] For immunoblot validation, we found that JNK signaling was highly enhanced in the liver of 31-KO mice. The total JNK was comparable, but the p-JNK, a pivotal molecule in JNK signaling, was higher in the liver of 31-KO mice than that of WT mice (Figure 5E). To confirm its JNK dependence, we also injected the specific p-JNK inhibitor SP600125 intraperitoneally, 1 hour before APAP administration, in both 31-KO and WT mice. Surprisingly, both groups showed normal hepatic transaminase levels at 24 hours after APAP administration (Figure 5F), and, accordingly, very mild hepatic necrosis and DNA fragmentation (Figure 5G). A previous study showed that translocation of p-JNK to mitochondrial Sab in hepatocytes leads to rapid dephosphorylation of Src, thus impairing mitochondrial function, which precedes necrotic cell death in APAP-induced liver injury.[5] We then determined these downstream molecules of JNK signaling in isolated mitochondria and found that p-JNK was increased and p-Src was decreased significantly in 31-KO mice, compared to that of WT mice (Figure 5H). This indicates an additional JNK translocation and mitochondrial dysfunction in 31-KO mice. Accordingly, ROS production also was increased dramatically in the hepatocytes of 31-KO than that of WT mice (Figure 5I). Our results indicate that the aggravated liver damage in 31-KO mice is attributable to enhanced JNK signaling activation and mitochondrial dysfunction.

miR-31 Directly Targeted Cdc42 in DILI

miRNA-mediated RNA translational repression can be accomplished via a slicing-competent Argonaute (Ago) protein to inhibit messenger RNA (mRNA) translation or cleave target mRNA in the RNA-induced silencing complex (RISC). To investigate the target genes regulated by miR-31, the primary hepatocytes isolated from WT and 31-KO mice 6 hours after APAP injection were subjected to Ago2 binding RNA immunoprecipitation to pull-down interacting RNA, followed by high-throughput RNA sequencing (Ago2-RIP-seq) (Figure 6A). Using the ABL in silico Random Clustering (ABLIRC) strategy,[21] the genes specific in WT mice hepatocytes were compared with that of 31-KO and considered as potential target genes. Further on, combining them with gene expression abundance and miRmap database prediction, we finally filtered out 26 target genes (Figure 6B), including an important JNK regulator gene: Cdc42.[22,23] As shown in the landscape of Ago2-bound peaks (Figure 6C), Cdc42 mRNA in WT hepatocytes was enriched significantly in Ago2-RNA cross-linking adducts, compared with that observed in 31-KO hepatocytes, indicating that Cdc42 was the target of miR-31.

Using immunoblotting, we confirmed that CDC42 expression was increased markedly both in liver tissues (Figure 6D) and hepatocytes (Figure 6E) derived from 31-KO mice, compared with that of WT mice. In addition, the expression of CDC42 in WT mice at 6 hours was significantly lower than 0 hour, compared with that of 31-KO mice, which also indicates up-regulated miR-31 alleviates liver damage by targeting Cdc42. CDC42 could induce activation loop phosphorylation of mixed lineage kinase (MLK3),[24] and MLK3 also has a critical role in JNK activation in acetaminophen-induced hepatotoxicity.[25] We found that both phosphorylation of MLK3 and downstream kinase mitogen-activated protein kinase kinase 4 were enhanced significantly in the liver of 31-KO mice, compared with that of WT mice (Figure 6F). We also detected expression of CDC42 and subsequent JNK signaling in mouse primary hepatocytes transfected with miR-31 mimic or inhibitor and treated with APAP. As expected, miR-31 overexpression significantly diminished CDC42 expression, MLK3 phosphorylation and subsequent JNK signaling activation, while miR-31 inhibition induced opposite effects, compared with negative control (Figure 6G).

Figure 2. (*See previous page*). Comparison of hepatic innate inflammation infiltration between 31-KO and WT mice after APAP administration. (*A*) Flow cytometry analysis including hepatic neutrophils, monocytes, and Kupffer cells both in APAP-induced 31-KO and WT liver injury mice. (*B* and *C*) Comparison of hepatic infiltrating inflammatory cells between 31-KO and WT mice at both (*B*) 6 hours and (*C*) 24 hours after APAP injection. n = 8 per group. Data are representative of means ± SD. *P < .05, 2-tailed Student *t* test. KC, Kupffer cell.

A

B

C

D
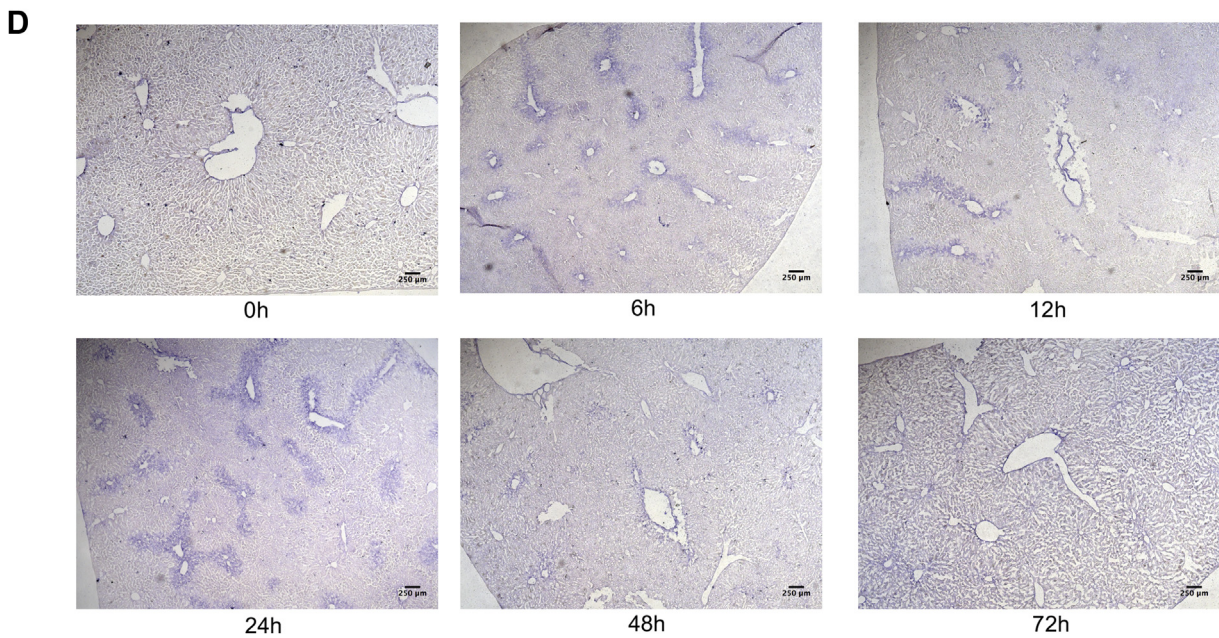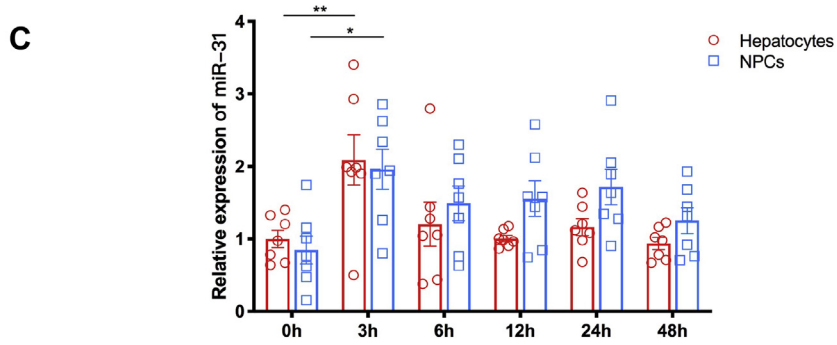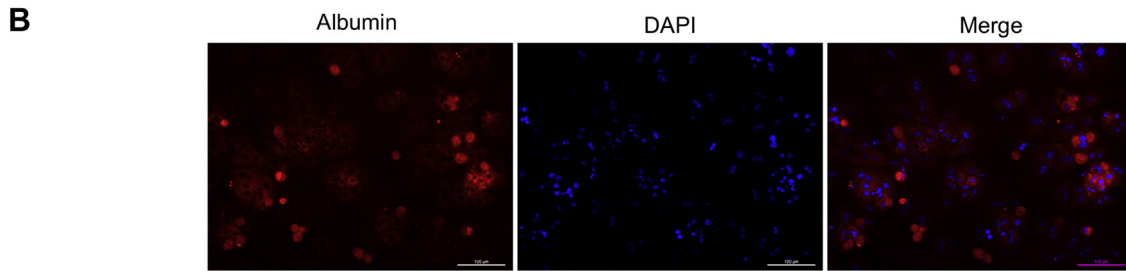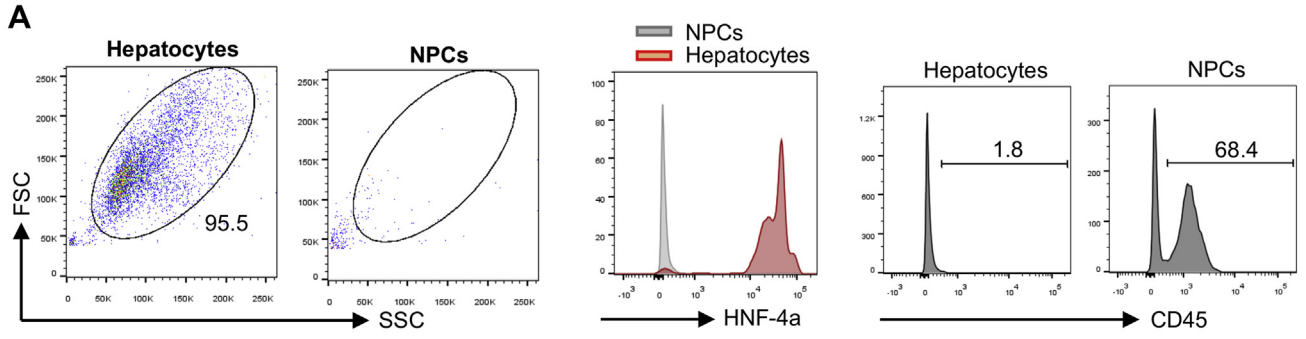
To further confirm whether Cdc42 is a direct target of miR-31, we generated luciferase reporter vectors containing the miR-31 binding site, or mutation site, in 3`-UTR sequence of Cdc42 mRNA. As shown in Figure 6H, with the augmentation of miR-31 transfection concentration, the restraint in luciferase activity became more and more significant, but the mutation of the seed sequence of the predicted miR-31 binding site abrogated this effect. To identify the role of Cdc42 in JNK signaling, we inhibited Cdc42 expression with specific small interfering RNA (siRNA) in mouse hepatocyte cell line AML-12 cells, resulting in significant diminishment of p-JNK at 6 hours after APAP administration (Figure 6I). Moreover, Cdc42 silencing mitigated the necrosis of hepatocytes after APAP treatment (Figure 6J). Taken together, these data suggest that Cdc42 is a functional miR-31 target and it has an important role in the activation of JNK signaling in APAP-induced DILI.

Up-regulation of miR-31 Was Induced by JNK Signaling in DILI

A previous study indicated that JNK signaling pathway activation could induce miR-31 expression.[17] Based on the earlier-described results, we hypothesized the existence of a negative feedback loop between JNK activation and miR-31 in APAP-induced DILI. We examined in vivo miR-31 expression in liver tissues after APAP injection, with or without treatment of JNK inhibitor, including a normal mice control group. APAP-treated mice injected with JNK inhibitor have shown a decreased level of miR-31 compared with APAP-treated mice, and even slightly lower than normal liver tissue (Figure 7A). For further validation, we also detected miR-31 expression in JNK activator anisomycin-treated primary hepatocytes (with or without JNK inhibitor SP600125) for 6 hours. As expected, miR-31 was enhanced in the group treated only with anisomycin, but not in the group treated together with both anisomycin and SP600125 (Figure 7B). Our whole model is summarized in Figure 7C.

miR-31 Also Was Highly Expressed in the Liver of Patients With DILI

Not only APAP induced intrinsic DILI, but idiosyncratic DILI also has been indicated as having a critical role in JNK signaling activation.[8] Clinically, because of different incidences and etiologies of DILI between mainland China and Western countries, in our study we included both intrinsic and idiosyncratic DILI cases (Table 1), including etiologies of acetaminophen (2 cases), antibiotic (1 cases), antituberculosis drug (1 case), ibuprofen (1 case), Chinese herb (5 cases), antiallergic agent (1 case), and a slimming drug (1 case) (Figure 8A). Noticeably, we found that hepatic JNK phosphorylation in DILI patients was higher than that of healthy controls (Figure 8B). As described in earlier results, miR-31 was induced by JNK activation in APAP-induced DILI. Therefore, we further examined the level of miR-31 in clinical samples and we found that miR-31 expression also was strongly increased in liver samples from DILI patients compared with healthy controls (Figure 8C). This indicates that the increase of miR-31 also is associated with JNK activation in human DILI.

Discussion

In the present study, we have shown a novel regulatory role of miR-31 in maintaining hepatic homeostasis in APAP-induced DILI. Mechanically, the up-regulation of miR-31 induced by JNK activation produces a negative feedback loop to limit JNK overactivation and mitochondrial dysfunction via suppressing small guanosine triphosphatase Cdc42, which protects hepatocytes from necrotic cell death.

As reported by studies from developed countries, acute liver failure is related mostly to acetaminophen overdose and idiosyncratic drug reactions,[26,27] whereas in mainland China, traditional Chinese medicine or herbal and dietary supplements are the major offending agents of DILI.[28] Most cases are highly individually differential and dose-independent. Therefore, we used a strategy to study the DILI regulatory mechanism with a more reproducible APAP-induced DILI mouse model then verification with clinical samples. Our results showed that APAP induced intrinsic DILI and traditional Chinese medicine–induced or other idiosyncratic DILI share a common mechanism in which activation of the JNK signaling pathway and mitochondrial dysfunction are critical events involved in cell death.[8] We found that in liver tissues from patients with DILI, both p-JNK and miR-31 were increased significantly, and this indicates that both miR-31 and JNK signaling play a critical role in DILI with different etiologies. However, because of the difficulty in obtaining clinical liver samples, those human samples were few and generally obtained from liver transplantation for acute liver failure, which means many days after the original drug overdose and the liver just did not recover. In the future, it will be of great interest to bring in more appropriate clinical DILI samples for further validation.

In past decades, the role played by the inflammatory cells in APAP-induced liver injury has raised an extensive concern.[29,30] Our previous study showed the immunoregulatory role of miR-31 in autoimmune disease.[13,31] However, via constructing bone marrow chimeric mice, we found that mice with miR-31 loss of function in a hematopoietic-derived immune system did not develop more severe liver

Figure 3. (*See previous page*). The expression profile of miR-31 in APAP-induced DILI. (A) Purity of hepatocytes and NPCs was analyzed by flow cytometry with a specific marker (hepatocyte nuclear factor 4 alpha (HNF-4a) or CD45). (B) Purity of hepatocytes also was validated by immunofluorescence staining with albumin. (C) Quantitative real-time polymerase chain reaction was used to detect the time course expression of miR-31 in parenchymal and nonparenchymal cells after APAP injection. n = 7 per group. (D) Using the miR-31–specific locked nucleic acid (LNA) probe, miRNA in situ hybridization was performed on liver tissue to observe the histologic time course expression of miR-31 in the APAP-induced DILI mouse model. Purple color indicates miR-31 expression. Data are representative of means ± SD. *P < .05, **P < .01, analysis of variance. DAPI, 4′,6-diamidino-2-phenylindole; FSC, forward scatter; SSC, side scatter.
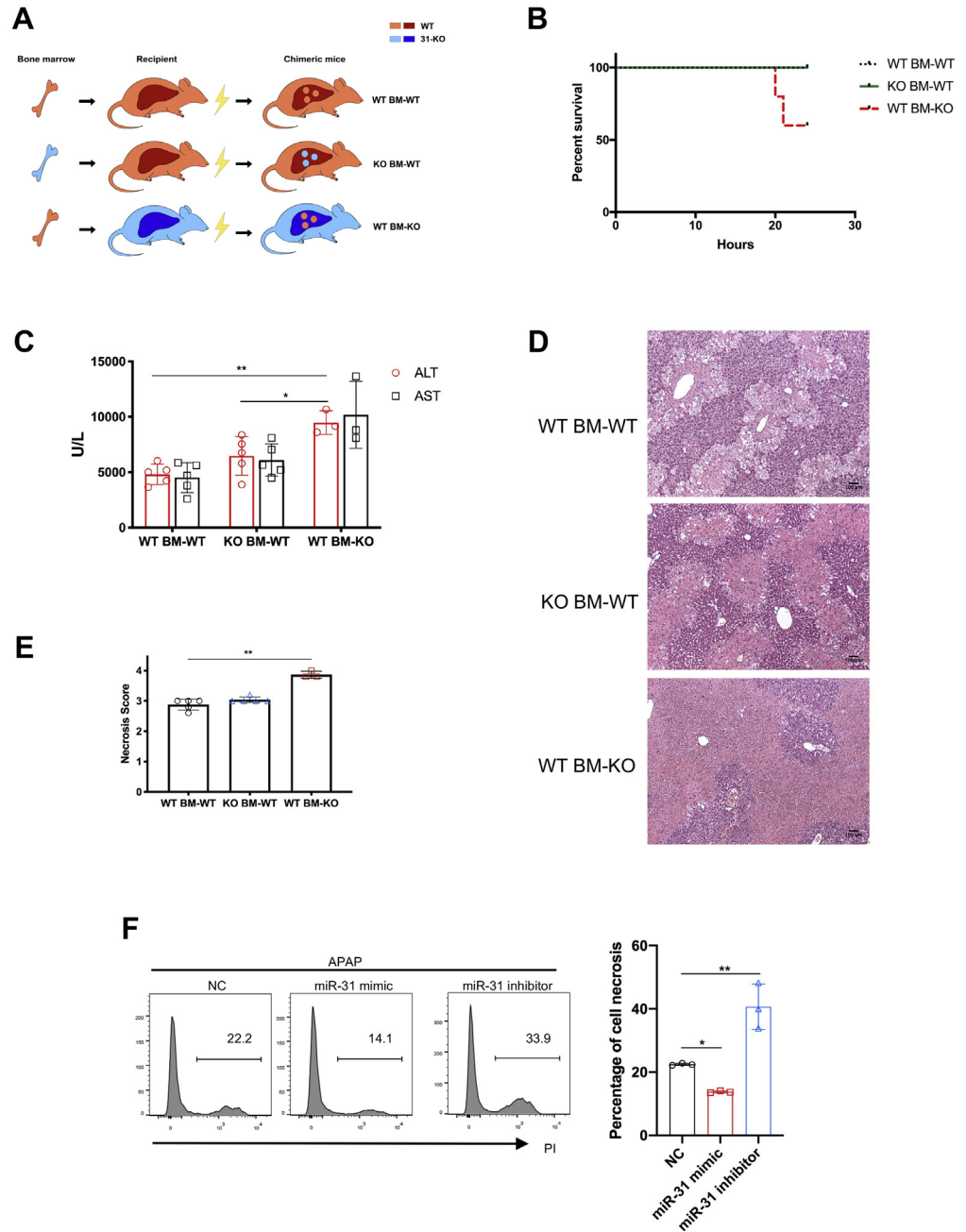
Figure 4. miR-31 exerted a protective role mainly via hepatocytes in APAP-induced DILI. (*A*) Schematic diagram of bone marrow chimeric mice construction. (*B*) Survival curve in bone marrow chimeric mice after APAP injection. n = 5 per group. (*C*) The level of serum ALT and AST in chimeric mice after 24 hours of APAP administration. n = 5 per group. (*D*) H&E staining of liver tissue from bone marrow chimeric mice after 24 hours of APAP administration. (*E*) Histologic necrosis analysis. n = 5 per group. (*F*) Primary hepatocytes transfected with miR-31 mimic, inhibitor, and negative control (NC) were treated with APAP for 6 hours, and cell necrosis was analyzed by flow cytometry. n = 3 per group. Data are representative of means ± SD. *P < .05 and **P < .01, 2-tailed Student *t* test or analysis of variance.

injury in APAP-induced DILI. This aspect precludes that miR-31 alleviates liver damage through infiltrating inflammatory cells. Therefore, highly infiltrated neutrophils in 31-KO mice are most likely to be caused by severe hepatocyte necrosis and just a critical event for inflammation resolution or clearance of hepatic debris.[32,33] However, our study is an acute early injury model, and future research needs to be implemented to investigate the role of miR-31 in a subpopulation of immune cells and in later stages of DILI.

RISC includes mature miRNA and Ago protein, and is the main place where miRNA exerts its function. RNA immunoprecipitation using Ago2-specific antibodies combined with high-throughput sequencing could greatly improve the accuracy and reduce the scope of identifying

the transcript targeted specifically by miRNA.[34] In the current study, after combining the results of RIP-seq with the bioinformatics analysis, we finally screened out the miR-31 target, Cdc42. Cdc42 is a member of the Rho family of small guanosine triphosphate-binding proteins that are playing integral roles in intracellular signaling pathways transduction. Earlier research showed that Cdc42 potently could induce JNK activation, and Cdc42 loss of function would inhibit signaling from cell surface receptors to JNK.[22,23] Cdc42 was also a major contributor to MLK3 activation in the saturated fatty acid–stimulated JNK signaling pathway in hepatocytes.[23] However, the role of Cdc42 has not yet been studied in APAP-induced DILI. In our results, the expression of Cdc42 was increased markedly both in the
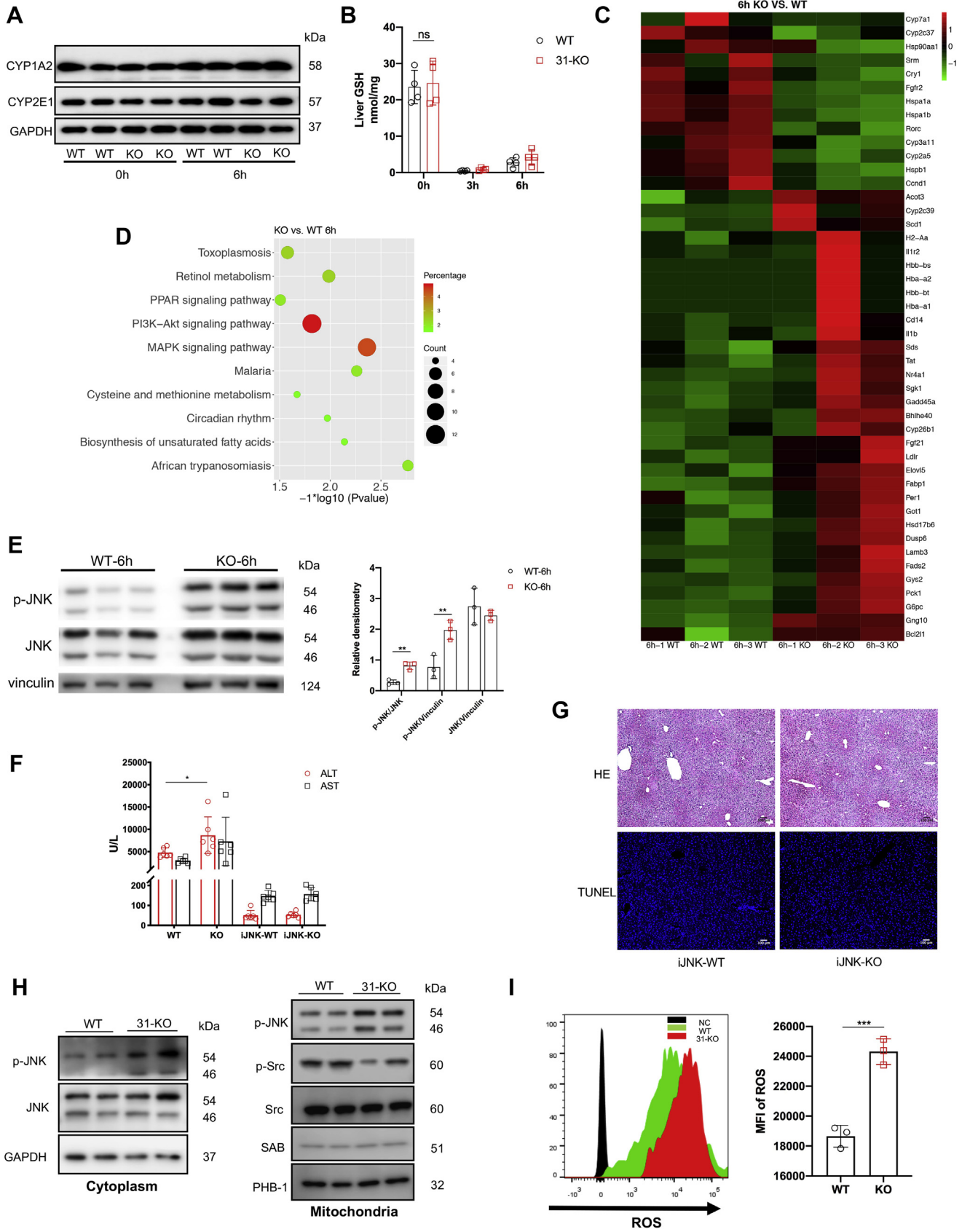
liver and hepatocyte of 31-KO mice after APAP injection, and Cdc42 inhibition by specific siRNA significantly decreased both JNK activation and necrosis in APAP-treated mice hepatocytes. Consistent with previous studies,[25,35] our study also confirmed that increased Cdc42 can enhance MLK3 phosphorylation and subsequent activation of downstream JNK signaling, aggravating hepatocyte injury in APAP hepatotoxicity. Although we have shown that miR-31 can directly target Cdc42 to regulate JNK signaling, miRNA is characterized by multitarget regulation, and there also may be other targets and pathways involved in DILI. JNK activation interacts with Sab to conduct intramitochondrial signaling, and miR-31 has been suggested to increase P53 signaling in cancer cells,[36] which in turn could repress expression of Sab.[37] The functional roles of miRNA in a particular tissue inevitably will be restricted because only a subset of its target genes is expressed.[38] We found that there was no significant difference of Sab expression in the mitochondria between 31-KO and WT mice, indicating that miR-31 modulates mitochondrial homeostasis mainly through the miR-31-Cdc42-MLK3 axis instead of P53.

An interesting point in our studies was that there is a safety mode, the feedback loop of JNK/miR-31/Cdc42, induced by JNK signaling itself, to maintain hepatocyte homeostasis in APAP-induced DILI. Although drug intake targeting JNK may be beneficial for the treatment of APAP-induced DILI, this also might include potential side effects. Indeed, JNK activated by other stimuli may lead to nonlethal pathophysiological or physiological consequences, such as insulin signaling, liver regeneration, and even tumor suppression.[39,40] Thus, we speculate that small-molecule miR-31 may be easier to be designed for drug delivery to enhance its therapeutic potential as a drug against APAP-induced DILI. Additional work is required to illustrate this intriguing speculation, and this might enrich the scarce therapeutic options in intrinsic or idiosyncratic DILI.

Materials and Methods
Animals

C57BL/6J mice were purchased from The Jackson Laboratory (Bar Harbor, ME). The miR-31 gene knockout (*miR-31$^{-/-}$*) mice were on a *C57BL/6* background. Male mice at 8–12 weeks of age were used in all experiments. The mice were kept under specific pathogen-free conditions, in compliance with the regulations of the Guide for the Care and Use of Laboratory Animals, upon Scientific Investigation Board approval (SYXK-2003-0026, Shanghai Jiao Tong University School of Medicine, Shanghai, China). To ameliorate any suffering in the mice observed throughout these experimental studies, the mice were killed by CO_2 inhalation.

Human Samples

The DILI liver samples were collected from transplant patients with acute liver failure and healthy control liver tissues were collected from living liver donors at Renji Hospital of Shanghai Jiao Tong University School of Medicine (Shanghai, China). Patients' clinical characteristics were analyzed, and are presented in Table 1. The present study was reviewed and approved by the Ethics Committee of Renji Hospital of Shanghai Jiao Tong University School of Medicine (Shanghai, China).

APAP-Induced DILI Mouse Model

All animals were fasted overnight for 16 hours before APAP treatment. APAP (Sigma-Aldrich, St. Louis, MO) was dissolved in warmed phosphate-buffered saline, and the animals were treated intraperitoneally with an APAP dosage of 300 mg/kg. Blood and liver samples were collected at various time points after APAP administration.

Isolation of Hepatic Parenchymal and Nonparenchymal Cells

A modification of the nonrecirculating 2-step in-situ perfusion method was applied.[41] In brief, liver was perfused through the portal vein using fresh solutions containing type IV collagenase. After sufficient digestion, the liver was excised and transferred to a sterile dish. Cells were stripped and filtered through a 70-μm stainless nylon strainer, and centrifuged at $50 \times g$ for 5 minutes. The resulting pellet contained hepatic parenchymal cells (primary hepatocytes). Supernatant fluids containing hepatic NPCs were centrifuged further at $450 \times g$ for 5 minutes.

Figure 5. (*See previous page*). **JNK signaling pathway and mitochondrial dysfunction were strongly enhanced in 31-KO mice.** (*A*) Expression of APAP metabolizing enzymes including cytochrome P450 isoforms 2 (CYP)2E1 and CYP1A2 were detected in the liver before and after APAP treatment. (*B*) Comparison of time course content of GSH in fresh liver between 31-KO and WT mice. n = 4 per group. (*C*) Heat map of hepatic differentially expressed mRNAs from the top 10 pathways between 31-KO and WT at 6 hours after APAP injection. (*D*) Kyoto Encyclopedia Genes and Genomes pathway analysis of differentially expressed genes between 31-KO and WT livers at 6 hours after APAP administration. (*E*) Comparison of JNK phosphorylation between 31-KO and WT mice at 6 hours after APAP injection. n = 3 per group. (*F*) Serum ALT and AST levels at 24 hours after APAP injection with or without SP600125 administration. n = 6 per group. (*G*) Comparison of H&E and terminal deoxynucleotidyl transferase–mediated deoxyuridine triphosphate nick-end labeling (TUNEL) (for DNA fragmentation) hepatic staining between 31-KO and WT mice at 24 hours after APAP injection with or without SP600125 administration. In TUNEL staining, red indicates DNA fragmentation and blue indicates 4′,6-diamidino-2-phenylindole nucleus. (*H*) Mitochondria and cytoplasm (removal of mitochondria) were isolated from liver tissue in 31-KO and WT mice 6 hours after APAP administration. Western blot analysis was performed using antibody against p-JNK, JNK, GAPDH, p-Src, Src, SAB, and PHB-1. (*I*) The detection of ROS production in hepatocytes isolated from 31-KO, WT mice 6 hours after APAP administration, and negative control (NC) also was set. n = 3 per group. Data are representative of means ± SD. *P < .05 and **P < .01, 2-tailed Student t test or analysis of variance. GAPDH, glyceraldehyde-3-phosphate dehydrogenase; iJNK, JNK inhibitor; MFI, Mean Fluorescence Intensity; PHB, Prohibitin; PI3K-Akt, phosphatidylinositol 3-kinase-protein kinase B; PPAR, peroxisome proliferator activated receptor.
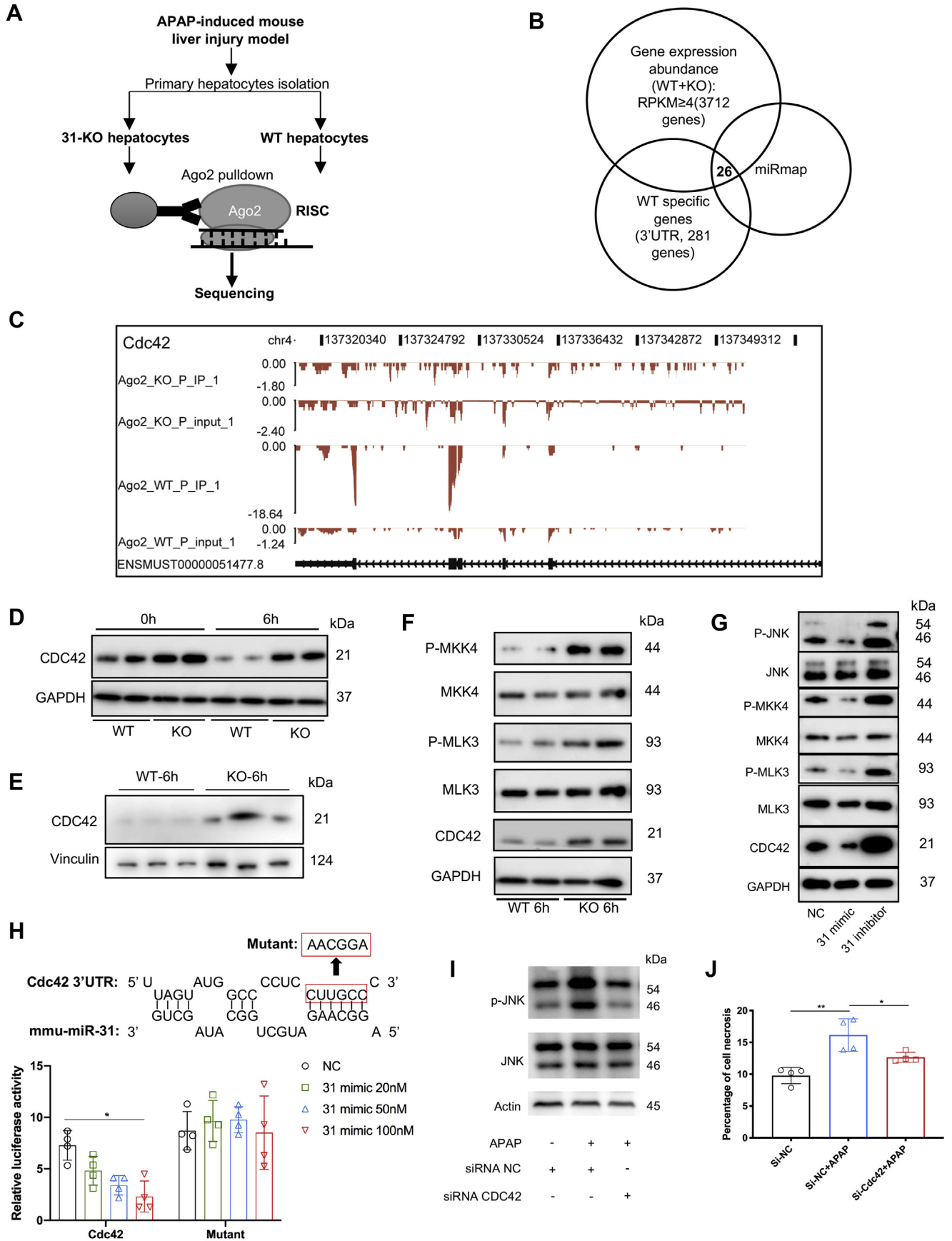
miR-31 Overexpression or Inhibition Cell Assay

Fresh isolated mouse primary hepatocytes were cultured in Dulbecco's modified Eagle medium/F-12 (Gibco, Gaithersburg, MD) and supplemented with heated-inactivated 10% fetal bovine serum (Gibco), penicillin, and streptomycin in an atmosphere of 5% CO_2 at 37°C overnight. Then mouse primary hepatocytes were transfected with miR-31 mimic (100 nmol/L) or miR-31 inhibitor (100 nmol/L) to overexpress or deplete miR-31, and NC control also was set. After 48 hours of transfection, primary hepatocytes were treated with 20 mmol/L APAP for 6 hours.

Transfection of siRNA and Cell Assay

The mouse hepatocyte AML-12 cell line was purchased from the Cell Bank of Type Culture Collection of the Chinese Academy of Science (Shanghai, China), and culture conditions were the same as described for the primary hepatocytes. Then, AML-12 cells were transfected with siRNA (GenePharma) targeting murine Cdc42 or control siRNA for 24 hours, followed by treatment with 20 mmol/L APAP for 6 hours. The siRNA sequence against Cdc42 was TCACACAGAAAGGCCTAAA.

Aminotransferase and Hepatic Pathology

The levels of serum ALT and AST were measured using an automatic analyzer (Hitachi 7180, Tokyo, Japan). For the histologic examination, the liver tissue was fixed (4% paraformaldehyde), paraffin-embedded, sectioned, and stained with H&E to determine morphologic changes. H&E-stained liver sections were examined under a regular microscope (100× total magnification, Axio scope A1; Zeiss [Jena, Germany]), and necrosis evaluation was graded using a system previously described[18,42]: 0, no lesion present; 1/2, individual necrotic cells seen at the first cell layer adjacent to the central vein, and hyaline degeneration present; 1, necrotic cells extending 2 or 3 cell layers from the central veins; 2, necrotic cells extending 3–6 cell layers from the central veins, but limited in peripheral distribution; 3, the same as 2, but with necrosis extending from one central vein to another; and 4, more severe than 3, with extensive centrilobular necrosis throughout the section. An overall score was computed for each liver section based on the assessment of 5 lobules.

RNA Reverse Transcription and Quantitative Polymerase Chain Reaction

Total RNA was extracted using the TRIzol reagent (Invitrogen, Carlsbad, CA). To measure mature miR-31 levels, 100 ng total RNA was reverse transcribed using the TaqMan miRNA reverse transcription kit (Thermo Scientific, MA, USA). Then, the complementary DNAs were analyzed by qPCR using the TaqMan probes designed for miR-31 and U6 in ViiA 7 facility (Applied Biosystems, MA, USA). Quantification of relative miRNA expression was measured by the comparative CT method ($2^{-\Delta\Delta CT}$), normalized to endogenous U6 expression.

Flow Cytometry Analysis

The hepatic leukocytes analysis procedure was adapted from a method previously described by Watanabe et al.[43] Briefly, redundant blood was removed through the ventriculus sinister perfusion with normal saline. Then the liver was immediately excised and pressed through a 70-μm stainless strainer. The cell suspension was centrifuged at 50 × g for 2 minutes to remove hepatocytes and large debris. Later, the supernatant containing leukocytes was centrifuged at 400 × g for 5 minutes, and ACK lysing buffer (Invitrogen) was used to lyse redundant erythrocyte. For flow cytometry analysis, 10^6 cells were first incubated for 20 minutes with Fcγ receptor blocking Ab (BD Pharmingen), then stained with antibodies at a concentration of 1 μg/100 μL for 30 minutes at 4°C, protected from light. Antibodies used in these experiments are listed in Supplementary Table 1. Finally, cells were washed, resuspended, assayed with BD LSRFortessa X-20 Flow Cytometer (Franklin Lakes, NJ), and analyzed with FlowJo X software 10.0.7 (FlowJo, Ashland, OR). For in vitro cell death analysis, we used PE Annexin V Apoptosis Detection Kit I (BD, Franklin Lakes, NJ) according to the manufacturer's instructions.

Reactive oxygen species (ROS) Detection

ROS were detected with CellROX Green Flow Cytometry Assay Kit (Invitrogen) according to the manufacturer's instructions. In brief, hepatocytes were isolated in situ perfusion at indicated time from APAP-induced injury mice as described earlier. The cells then were incubated in cell-

Figure 6. (*See previous page*). **Ago2-RIP-Seq identified target of miR-31.** (*A*) Experimental workflow of the Ago2-RIP-Seq experiment. (*B*) Screening strategy of miR-31–specific target genes. (*C*) The normalized reads density landscape of Ago2-bound peaks on Cdc42 from RIP-seq. (*D*) Western blot analysis of Cdc42 expression in liver tissues of WT and 31-KO mice at 0 or 6 hours after APAP injection. (*E*) Western blot analysis of Cdc42 expression in hepatocytes derived from WT and 31-KO mice at 6 hours after APAP injection. n = 3 mice per group. (*F*) Phosphorylation of upstream JNK signaling including p-MKK4 and p-MLK3 were detected in the livers of 31-KO and WT mice 6 hours after APAP injection. (*G*) Primary hepatocytes transfected with miR-31 mimic, inhibitor, and NC control were treated with APAP for 6 hours, then CDC42 and respective molecules of JNK signaling were detected in Western blot. (*H*) Overall matching targets between Cdc42 3' untranslated region (UTR) and miR-31 were presented by RNAhybrid. Luciferase activity was determined in NIH3T3 cells that were transfected with the Cdc42 3'UTR reporter construct or mutant control with different concentrations of miR-31 mimics or NC. n = 4 per group. (*I*) Western blot analysis of p-JNK, JNK, and actin in AML-12 cells transfected with siRNA NC or siRNA Cdc42 in the presence of APAP for 6 hours, and (*J*) cell necrosis was analyzed with flow cytometry. Data are representative of means ± SD. *P < .05, **P < .01, 2-tailed Student t test or analysis of variance (ANOVA). GAPDH, glyceraldehyde-3-phosphate dehydrogenase; NC, negative control; p-MLK3, phosphorylated mixed-lineage kinase 3; p-MKK4, phosphorylated mitogen-activated protein kinase kinase 4; RISC, RNA-induced silencing complex; RPKM, Reads Per Kilobase per Million mapped reads; Si, siRNA.
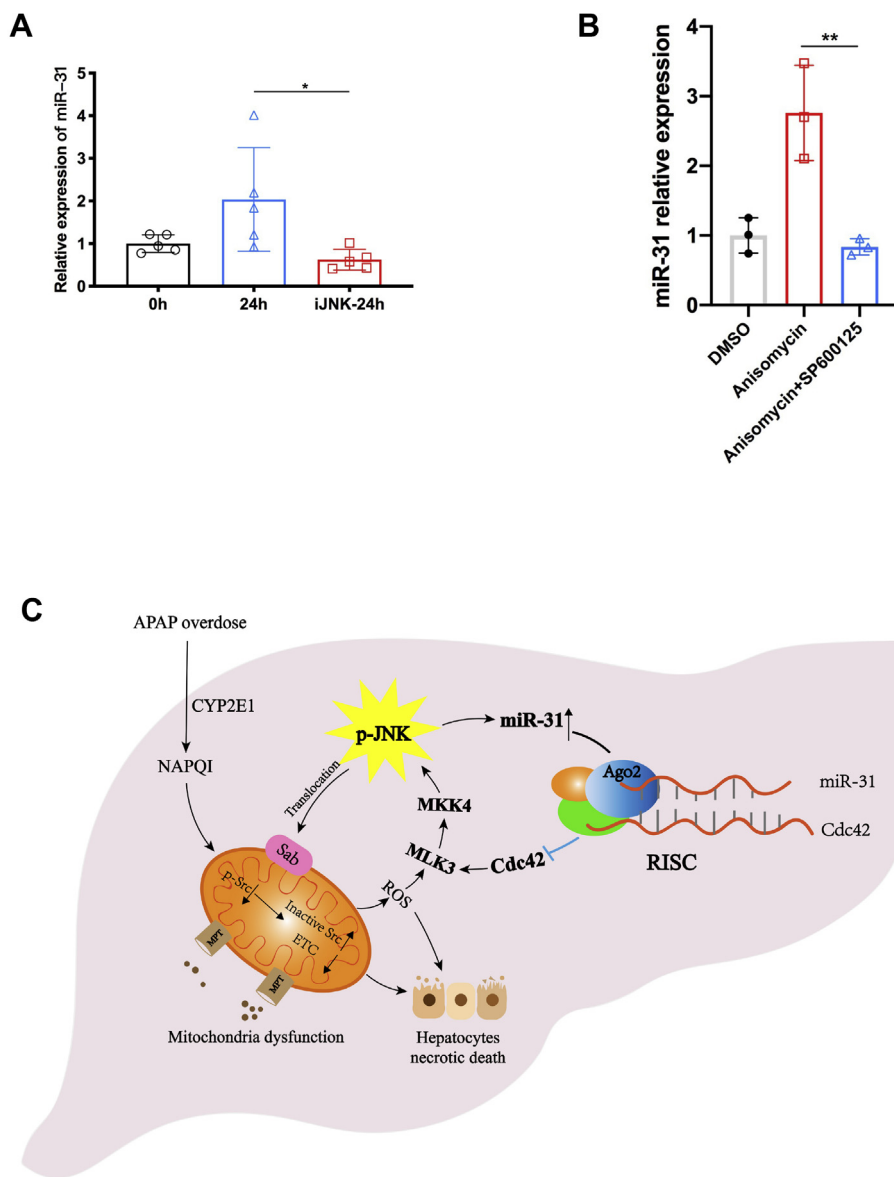
Figure 7. The up-regulation of miR-31 was induced by JNK activation. (*A*) miR-31 expression was detected in the liver at 24 hours after in vivo administration of APAP or JNK inhibitor. n = 5 mice per group. (*B*) The expression level of miR-31 was detected in primary hepatocytes stimulated with JNK activator (anisomycin) or JNK inhibitor (SP600125) for 6 hours. n = 3 per group. (*C*) The proposed model of our present study. Data are representative of means ± SD. *$P < .05$, **$P < .01$, 2-tailed Student t test or analysis of variance. DMSO, dimethyl sulfoxide; iJNK, JNK inhibitor; MLK, mixed-lineage kinase; MKK, mitogen-activated protein kinase kinase; MPT, mitochondrial permeability transition; NAPQI, N-acetyl-p-benzoquinone imine; RISC, RNA-induced silencing complex.

permeable, peroxide-sensitive fluorophore CellROX Green reagent for 30 minutes at 37°C, protected from light and analyzed on BD LSRFortessa X-20 Flow Cytometer (Franklin Lakes, NJ).

In Situ Hybridization

In situ hybridization was performed on 10-μm–thick frozen sections of liver specimens, using the method previously described.[44] The 5'-DIG and 3'-DIG-labeled miRCURY LNA detection probe designed for mmu-miR-31-5p was purchased from Exiqon (Copenhagen, Denmark).

Generation of Bone Marrow Chimeric Mice

Bone marrow cells were flushed from miR-31$^{-/-}$ or wild-type donor mice. Erythrocyte-depleted bone marrow cells were adoptively transferred into lethally irradiated (900 rads) wild-type mice or miR-31$^{-/-}$ mice (8-week-old, 5×10^6-1×10^7 cells per mouse). Totally three groups were set (Figure 4*A*): KO bone marrow transferred to WT recipient (KO BM-WT), WT bone marrow transferred to KO recipient (WT BM-KO), and WT bone marrow transferred to WT mice (WT BM-WT). After 8 weeks, the chimeric mice were subjected to APAP-induced DILI mouse model.

RNA-Seq and Data Analysis

Liver tissues from WT and 31-KO mice post-APAP injection were collected for total RNA extraction. Complementary DNA library was constructed and sequenced on an Illumina Hiseq4000 Platform. The expression levels of each transcript were calculated according to the fragments per kilobase of exon per million mapped reads (FPKM

Table 1. Demographic Data of Patients With DILI

Characteristic	DILI	Normal control
Sex		
Male	6	4
Female	6	4
Age at LT, *mo*	504 (435–657)	336 (324–432)
Etiology		
Acetaminophen	2	
Antibiotic	1	
Ibuprofen	1	
Antituberculosis drug	1	8 (donor of LDLT)
Chinese herb	5	
Antiallergic drug	1	
Slimming drug	1	

NOTE. The values in parentheses represent 25% and 75% percentiles.
LT, living donor liver transplantation.

method). Genes with a variation of at least 1.8-fold and *P* value less than .05 compared with relative samples, were considered as DEGs. In addition, significant DEGs were used for Kyoto Encyclopedia Genes and Genomes analysis, which was performed using DAVID 6.8 (http://david.ncifcrf.gov). The primary raw data have been deposited in the Sequence Read Archive of NCBI, and accession numbers are between SRR11262768 and SRR11262773.

Ago2-RNA Immunoprecipitation Combined With High-Throughput Sequencing (Ago2-RIP-seq)

Primary hepatocytes isolated from WT and 31-KO mice, 6 hours after APAP injection, were irradiated once for 400 mJ/cm^2 and lysed in ice-cold lysis buffer with RNase inhibitor and a protease inhibitor. Then, RNA qualified (RQ) I DNase, micrococcal nuclease (MNase), and the mixture were vibrated vigorously and centrifuged to remove cell debris. The supernatant was incubated with DynaBeads protein G (Thermo) conjugated with anti-Ago2 antibody (Abnova, Taipei, China). The Ago2-bound RNAs were isolated from the immunoprecipitation (IP) of anti-Ago2 using TRIzol (Invitrogen, Carlsbad, CA). Total RNA of hepatocytes, which was set as input control, also was isolated using TRIzol. Complementary DNA libraries were prepared with the KAPA RNA Hyper Prep Kit (KAPA, Boston, MA) according to the manufacturer's procedure. High-throughput sequencing of the complementary DNA libraries was performed on an Illumina Xten (California, CA) platform for 150 bp paired-end sequencing.

RIP-Seq Peak Calling Analysis

After reads were aligned onto the genome, only uniquely mapped reads were used for analysis. The ABL in silico Random Clustering (ABLIRC) strategy was used to identify the binding regions of Ago2 on the genome.[21] Reads with at least 1 bp overlap were clustered as peaks. For each gene, computational simulation was used to randomly generate reads with the same number and lengths as reads in peaks.

The outputting reads were further mapped to the same genes to generate random maximum peak height from overlapping reads. The whole process was repeated 500 times. All of the observed peaks with heights higher than those of random maximum peaks ($P < .05$) were selected. The immunoprecipitation (IP) and input control were analyzed by the simulation independently, and the IP peaks that overlapped with input peaks were removed. The target genes of IP were finally determined by the peaks. The primary raw data have been deposited in the Sequence Read Archive of National Center for Biotechnology Information (NCBI), and accession numbers are between SRR11263243 and SRR11263246.

Terminal Deoxynucleotidyl Transferase–Mediated Deoxyuridine Triphosphate Nick-End Labeling Assay

The detection of DNA fragmentation was performed by a terminal deoxynucleotidyl transferase–mediated deoxyuridine triphosphate nick-end labeling assay using a commercially available kit (In Situ Cell Death Detection Kit, TMR red; Roche, Basel, Switzerland) following the manufacturer's instructions. In brief, the paraffin-embedded liver sections were treated with proteinase K (20 μg/mL) for 20 minutes after dewaxing and hydration, then a reaction mix was added to the liver tissue for 1 hour at room temperature. The positive terminal deoxynucleotidyl transferase–mediated deoxyuridine triphosphate nick-end labeling and 4′,6-diamidino-2-phenylindole staining were observed under a fluorescence microscope (Zeiss, Jena, Germany).

Immunofluorescence

Mouse primary hepatocytes were subjected to immunofluorescent staining as previously described.[45] The antibody used was mouse anti-albumin antibody (sc-271605; Santa Cruz, Dallas, TX).
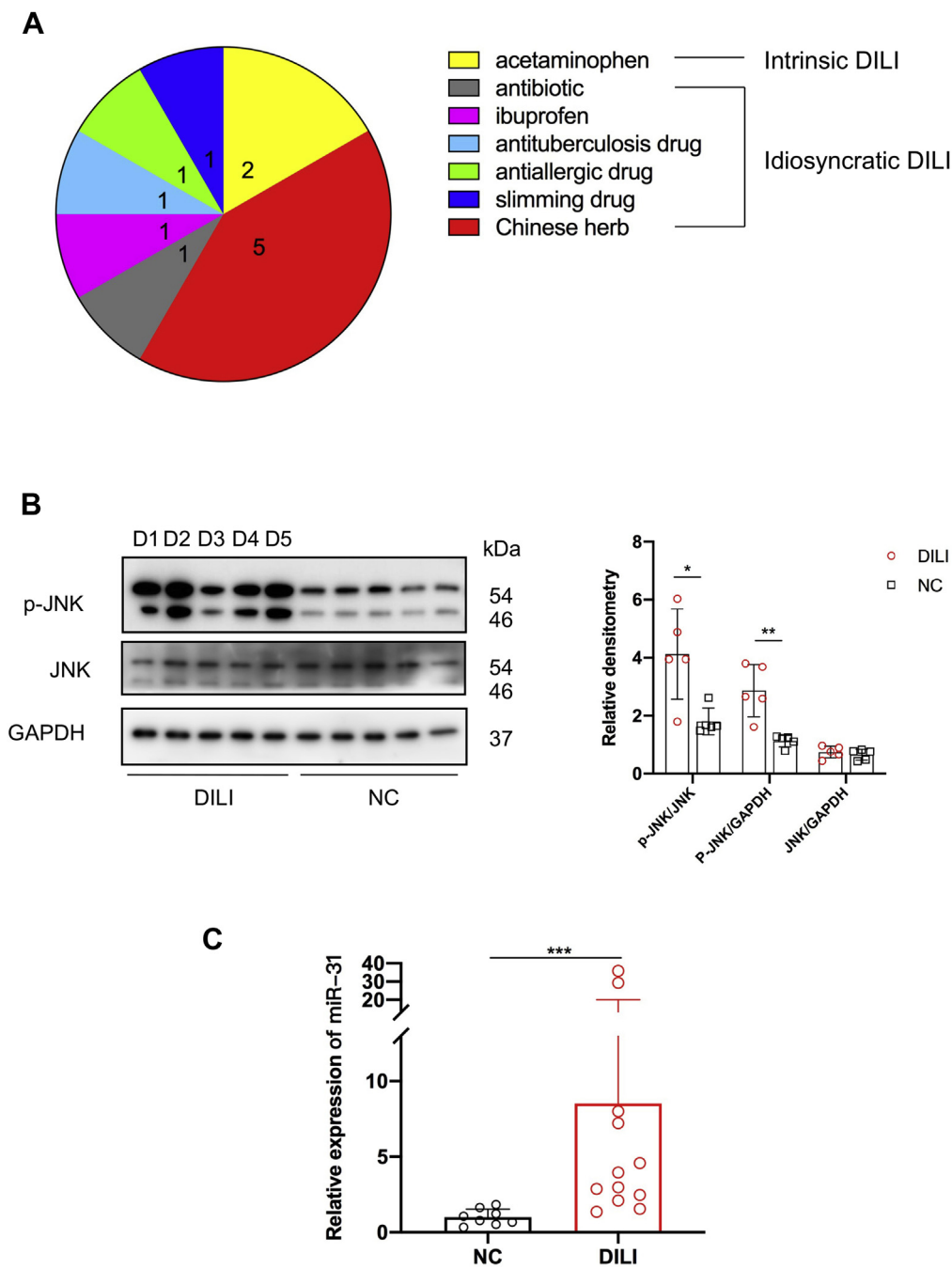
Isolation of Mitochondria From Liver Tissue

A tissue mitochondrial extraction kit (Beyotime, Shanghai, China) was used for mitochondria isolation from fresh liver tissue according to the manufacturer's instructions. The freshly isolated mitochondria and corresponding cytoplasm were immediately subjected to protein extraction.

Western Blot

Samples were lysed in RIPA lysis buffer (Beyotime) and supplemented with a protease and phosphatase inhibitor cocktail (Thermo Scientific, Waltham, MA). Antibodies applied in these experiments are listed in Supplementary Table 1. The band was detected with ECL Western Blotting Substrate (Beyotime) by a GE Amersham Imager 600 (GE, Fairfield, CT).

Administration of JNK Inhibitor SP600125

The mice were treated with JNK-specific inhibitor SP600125 (MedChemExpress, Monmouth Junction, NJ) at 15

A

legend:
- acetaminophen —— Intrinsic DILI
- antibiotic
- ibuprofen
- antituberculosis drug
- antiallergic drug — Idiosyncratic DILI
- slimming drug
- Chinese herb —

B

C

Figure 8. Both JNK activation and miR-31 expression were increased in the liver from patients with DILI. (*A*) Etiologies of DILI patients. (*B*) Comparison of JNK phosphorylation in liver samples between representative DILI patients and normal controls. n = 5. Etiologies of DILI included erythromycin (D1), ibuprofen (D2), antituberculosis drugs (D3), acetaminophen (D4), and Chinese herb (D5). NC, normal control. (*C*) Comparison of miR-31 expression in liver samples between DILI patients and normal controls. n = 8–12. Data are representative of means ± SD. *$P < .05$, **$P < .01$, 2-tailed Student t test. GAPDH, glyceraldehyde-3-phosphate dehydrogenase.

mg/kg dissolved in 5% dimethyl sulfoxide and 95% corn oil or the same volume vehicle control (5% dimethyl sulfoxide and 95% corn oil) intraperitoneally, 60 minutes before APAP administration. After treatment, mice were analyzed for aminotransferase, histology, and miR-31 expression.

Luciferase Assays

The 3' untranslated region fragments of Cdc42 and mutant control were cloned into psiCHECK-2 vector (Promega, Madison, WI). Mouse embryonic fibroblast cells (NIH3T3 cells) were cultured in Dulbecco's modified Eagle medium high-glucose medium (Thermo Scientific) supplemented with 10% fetal bovine serum (Gibco) in an atmosphere of 5% CO_2 at 37°C. Cells with 60%–90% confluence were co-transfected with 100 ng dual luciferase reporter vector and different concentrations (20, 50, or 100 nmol/L) of miR-31 mimics (GenePharma) using Lipofectamine3000 (Thermo Scientific). The cells were lysed 24 hours after transfection and luciferase activity was measured using the Dual-Luciferase Reporter Assay System (Promega) on a microplate reader (Berthold, Bad Wildbad, Germany). The renilla:firefly luciferase ratio was calculated for each well.

Measurement of Liver Tissue Glutathione Level

Fresh liver tissues were collected from 31-KO or WT mice at indicated times after APAP injection. Then, the liver tissue glutathione level was detected using the Total Glutathione Assay Kit (Beyotime) according to the manufacturer's instructions.

Statistical Analysis

The data were analyzed with GraphPad Prism 7 (GraphPad Software, Inc, La Jolla, CA) and were presented as the means $\pm$ SD. The Student t test was used to compare 2 conditions, and analysis of variance was used for multiple comparisons. Clinical demographic data were compared with the chi-square test. Probability values were indicated and considered significant when less than <0.05.

All authors had access to the study data and reviewed and approved the final manuscript.

References

1. Jozwiak-Bebenista M, Nowak JZ. Paracetamol: mechanism of action, applications and safety concern. Acta Pol Pharm 2014;71:11–23.
2. Du K, Ramachandran A, Jaeschke H. Oxidative stress during acetaminophen hepatotoxicity: sources, pathophysiological role and therapeutic potential. Redox Biol 2016;10:148–156.
3. Yan M, Huo Y, Yin S, Hu H. Mechanisms of acetaminophen-induced liver injury and its implications for therapeutic interventions. Redox Biol 2018; 17:274–283.
4. Raucy JL, Lasker JM, Lieber CS, Black M. Acetaminophen activation by human liver cytochromes P450IIE1 and P450IA2. Arch Biochem Biophys 1989;271: 270–283.
5. Win S, Than TA, Min RW, Aghajan M, Kaplowitz N. c-Jun N-terminal kinase mediates mouse liver injury through a novel Sab (SH3BP5)-dependent pathway leading to inactivation of intramitochondrial Src. Hepatology 2016; 63:1987–2003.
6. Bajt ML, Cover C, Lemasters JJ, Jaeschke H. Nuclear translocation of endonuclease G and apoptosis-inducing factor during acetaminophen-induced liver cell injury. Toxicol Sci 2006;94:217–225.
7. McGill MR, Sharpe MR, Williams CD, Taha M, Curry SC, Jaeschke H. The mechanism underlying acetaminophen-induced hepatotoxicity in humans and mice involves mitochondrial damage and nuclear DNA fragmentation. J Clin Invest 2012;122:1574–1583.
8. Han D, Dara L, Win S, Than TA, Yuan L, Abbasi SQ, Liu ZX, Kaplowitz N. Regulation of drug-induced liver injury by signal transduction pathways: critical role of mitochondria. Trends Pharmacol Sci 2013;34:243–253.
9. Howell LS, Ireland L, Park BK, Goldring CE. MiR-122 and other microRNAs as potential circulating biomarkers of drug-induced liver injury. Expert Rev Mol Diagn 2018; 18:47–54.
10. He Y, Feng D, Li M, Gao Y, Ramirez T, Cao H, Kim SJ, Yang Y, Cai Y, Ju C, Wang H, Li J, Gao B. Hepatic mitochondrial DNA/Toll-like receptor 9/MicroRNA-223 forms a negative feedback loop to limit neutrophil overactivation and acetaminophen hepatotoxicity in mice. Hepatology 2017;66:220–234.
11. Chowdhary V, Teng KY, Thakral S, Zhang B, Lin CH, Wani N, Bruschweiler-Li L, Zhang XL, James L, Yang DK, Junge N, Bruschweiler R, Lee WM, Ghoshal K. miRNA-122 protects mice and human hepatocytes from acetaminophen toxicity by regulating cytochrome P450 family 1 subfamily A member 2 and family 2 subfamily E member 1 expression. Am J Pathol 2017;187: 2758–2774.
12. Yan S, Xu Z, Lou F, Zhang L, Ke F, Bai J, Liu Z, Liu J, Wang H, Zhu H, Sun Y, Cai W, Gao Y, Su B, Li Q, Yang X, Yu J, Lai Y, Yu XZ, Zheng Y, Shen N, Chin YE, Wang H. NF-kappaB-induced microRNA-31 promotes epidermal hyperplasia by repressing protein phosphatase 6 in psoriasis. Nat Commun 2015;6:7652.
13. Zhang L, Ke F, Liu Z, Bai J, Liu J, Yan S, Xu Z, Lou F, Wang H, Zhu H, Sun Y, Cai W, Gao Y, Li Q, Yu XZ, Qian Y, Hua Z, Deng J, Li QJ, Wang H. MicroRNA-31 negatively regulates peripherally derived regulatory T-cell generation by repressing retinoic acid-inducible protein 3. Nat Commun 2015;6:7639.
14. Tian Y, Ma X, Lv C, Sheng X, Li X, Zhao R, Song Y, Andl T, Plikus MV, Sun J, Ren F, Shuai J, Lengner CJ, Cui W, Yu Z. Stress responsive miR-31 is a major modulator of mouse intestinal stem cells during regeneration and tumorigenesis. Elife 2017;6:e29538.
15. Li J, Lv H, Che YQ. Upregulated microRNA-31 inhibits oxidative stress-induced neuronal injury through the JAK/STAT3 pathway by binding to PKD1 in mice with ischemic stroke. J Cell Physiol 2020;235:2414–2428.
16. Shi J, Ma X, Su Y, Song Y, Tian Y, Yuan S, Zhang X, Yang D, Zhang H, Shuai J, Cui W, Ren F, Plikus MV, Chen Y, Luo J, Yu Z. MiR-31 Mediates inflammatory signaling to promote re-epithelialization during skin wound healing. J Invest Dermatol 2018;138:2253–2263.
17. Zhong L, Simoneau B, Huot J, Simard MJ. p38 and JNK pathways control E-selectin-dependent extravasation of colon cancer cells by modulating miR-31 transcription. Oncotarget 2017;8:1678–1687.
18. Gunawan BK, Liu ZX, Han D, Hanawa N, Gaarde WA, Kaplowitz N. c-Jun N-terminal kinase plays a major role in murine acetaminophen hepatotoxicity. Gastroenterology 2006;131:165–178.
19. Henderson NC, Pollock KJ, Frew J, Mackinnon AC, Flavell RA, Davis RJ, Sethi T, Simpson KJ. Critical role of c-jun (NH2) terminal kinase in paracetamol- induced acute liver failure. Gut 2007;56:982–990.
20. Kyriakis JM, Avruch J. Mammalian MAPK signal transduction pathways activated by stress and inflammation: a 10-year update. Physiol Rev 2012;92:689–737.
21. Xia H, Chen D, Wu Q, Wu G, Zhou Y, Zhang Y, Zhang L. CELF1 preferentially binds to exon-intron boundary and regulates alternative splicing in HeLa cells. Biochim Biophys Acta Gene Regul Mech 2017;1860:911–921.

22. Coso OA, Chiariello M, Yu JC, Teramoto H, Crespo P, Xu N, Miki T, Gutkind JS. The small GTP-binding proteins Rac1 and Cdc42 regulate the activity of the JNK/SAPK signaling pathway. Cell 1995;81:1137–1146.

23. Sharma M, Urano F, Jaeschke A. Cdc42 and Rac1 are major contributors to the saturated fatty acid-stimulated JNK pathway in hepatocytes. J Hepatol 2012;56:192–198.

24. Du Y, Bock BC, Schachter KA, Chao M, Gallo KA. Cdc42 induces activation loop phosphorylation and membrane targeting of mixed lineage kinase 3. J Biol Chem 2005; 280:42984–42993.

25. Sharma M, Gadang V, Jaeschke A. Critical role for mixed-lineage kinase 3 in acetaminophen-induced hepatotoxicity. Mol Pharmacol 2012;82:1001–1007.

26. Ostapowicz G, Fontana RJ, Schiodt FV, Larson A, Davern TJ, Han SH, McCashland TM, Shakil AO, Hay JE, Hynan L, Crippin JS, Blei AT, Samuel G, Reisch J, Lee WM. US Acute Liver Failure Study Group. Results of a prospective study of acute liver failure at 17 tertiary care centers in the United States. Ann Intern Med 2002; 137:947–954.

27. Andrade RJ, Chalasani N, Bjornsson ES, Suzuki A, Kullak-Ublick GA, Watkins PB, Devarbhavi H, Merz M, Lucena MI, Kaplowitz N, Aithal GP. Drug-induced liver injury. Nat Rev Dis Primers 2019;5:58.

28. Shen T, Liu Y, Shang J, Xie Q, Li J, Yan M, Xu J, Niu J, Liu J, Watkins PB, Aithal GP, Andrade RJ, Dou X, Yao L, Lv F, Wang Q, Li Y, Zhou X, Zhang Y, Zong P, Wan B, Zou Z, Yang D, Nie Y, Li D, Wang Y, Han X, Zhuang H, Mao Y, Chen C. Incidence and etiology of drug-induced liver injury in mainland China. Gastroenterology 2019; 156:2230–2241 e11.

29. Jaeschke H, Williams CD, Ramachandran A, Bajt ML. Acetaminophen hepatotoxicity and repair: the role of sterile inflammation and innate immunity. Liver Int 2012;32:8–20.

30. Krenkel O, Mossanen JC, Tacke F. Immune mechanisms in acetaminophen-induced acute liver failure. Hepatobiliary Surg Nutr 2014;3:331–343.

31. Sole C, Domingo S, Ferrer B, Moline T, Ordi-Ros J, Cortes-Hernandez J. MicroRNA expression profiling identifies miR-31 and miR-485-3p as regulators in the pathogenesis of discoid cutaneous lupus. J Invest Dermatol 2019;139:51–61.

32. Lawson JA, Farhood A, Hopper RD, Bajt ML, Jaeschke H. The hepatic inflammatory response after acetaminophen overdose: role of neutrophils. Toxicol Sci 2000;54:509–516.

33. Williams CD, Bajt ML, Farhood A, Jaeschke H. Acetaminophen-induced hepatic neutrophil accumulation and inflammatory liver injury in CD18-deficient mice. Liver Int 2010;30:1280–1292.

34. Tichy D, Pickl JMA, Benner A, Sultmann H. Experimental design and data analysis of Ago-RIP-Seq experiments for the identification of microRNA targets. Brief Bioinform 2018;19:918–929.

35. Bock BC, Vacratsis PO, Qamirani E, Gallo KA. Cdc42-induced activation of the mixed-lineage kinase SPRK in vivo. Requirement of the Cdc42/Rac interactive binding motif and changes in phosphorylation. J Biol Chem 2000;275:14231–14241.

36. Creighton CJ, Fountain MD, Yu Z, Nagaraja AK, Zhu H, Khan M, Olokpa E, Zariff A, Gunaratne PH, Matzuk MM, Anderson ML. Molecular profiling uncovers a p53-associated role for microRNA-31 in inhibiting the proliferation of serous ovarian carcinomas and other cancers. Cancer Res 2010;70:1906–1915.

37. Win S, Min RW, Chen CQ, Zhang J, Chen Y, Li M, Suzuki A, Abdelmalek MF, Wang Y, Aghajan M, Aung FW, Diehl AM, Davis RJ, Than TA, Kaplowitz N. Expression of mitochondrial membrane-linked SAB determines severity of sex-dependent acute liver injury. J Clin Invest 2019;129:5278–5293.

38. Zhu W, Yang L, Du Z. MicroRNA regulation and tissue-specific protein interaction network. PLoS One 2011;6: e25394.

39. Cellurale C, Weston CR, Reilly J, Garlick DS, Jerry DJ, Sluss HK, Davis RJ. Role of JNK in a Trp53-dependent mouse model of breast cancer. PLoS One 2010; 5:e12469.

40. Saxena NK, Fu PP, Nagalingam A, Wang J, Handy J, Cohen C, Tighiouart M, Sharma D, Anania FA. Adiponectin modulates C-jun N-terminal kinase and mammalian target of rapamycin and inhibits hepatocellular carcinoma. Gastroenterology 2010;139:1762–1773, 73 e1–5.

41. Klaunig JE, Goldblatt PJ, Hinton DE, Lipsky MM, Chacko J, Trump BF. Mouse liver cell culture. I. Hepatocyte isolation. In Vitro 1981;17:913–925.

42. Wood M, Berman ML, Harbison RD, Hoyle P, Phythyon JM, Wood AJ. Halothane-induced hepatic necrosis in triiodothyronine-pretreated rats. Anesthesiology 1980;52:470–476.

43. Watanabe H, Ohtsuka K, Kimura M, Ikarashi Y, Ohmori K, Kusumi A, Ohteki T, Seki S, Abo T. Details of an isolation method for hepatic lymphocytes in mice. J Immunol Methods 1992;146:145–154.

44. Obernosterer G, Martinez J, Alenius M. Locked nucleic acid-based in situ detection of microRNAs in mouse tissue sections. Nat Protoc 2007; 2:1508–1514.

45. Wen Y, Feng D, Wu H, Liu W, Li H, Wang F, Xia Q, Gao WQ, Kong X. Defective initiation of liver regeneration in osteopontin-deficient mice after partial hepatectomy due to insufficient activation of IL-6/Stat3 pathway. Int J Biol Sci 2015;11:1236–1247.

Correspondence
Address correspondence to: Feng Xue, PhD, Department of Liver Surgery and Liver Transplantation Center, Renji Hospital, Shanghai Jiao Tong University School of Medicine, No. 160 Pujian Road, Shanghai 200127, China. e-mail: liversurgery6108_rj@sjtu.edu.cn; fax: (86) 21-58737232; or Honglin Wang, PhD, Center for Microbiota and Immunological Diseases, Shanghai General Hospital, Shanghai Institute of Immunology, Shanghai Jiao Tong University School of Medicine, No. 280 Chongqing Road, Shanghai 200025, China. e-mail: honglin.wang@sjtu.edu.cn; fax: (86) 21-6466099; or Yuanjia Tang, PhD, Shanghai Institute of Rheumatology, Renji Hospital, Shanghai Jiao Tong University School of Medicine, No. 145 Shandong (M) Road, Shanghai, 200001, China. e-mail: yjtang@sibs.ac.cn; fax: (86) 21-58752345.

performing miR-31 in situ hybridization, flow cytometry and bone marrow chimeric mice.

CRediT Authorship Contributions

Jianxin Zheng, MD (Conceptualization: Lead; Data curation: Lead; Formal analysis: Lead; Investigation: Lead; Methodology: Lead; Project administration: Lead; Resources: Lead; Software: Lead; Validation: Lead; Visualization: Lead; Writing – original draft: Lead)

Hong Zhou (Conceptualization: Equal; Data curation: Equal; Formal analysis: Equal; Investigation: Equal; Methodology: Lead; Validation: Lead; Writing – review & editing: Supporting)

Taihua Yang (Conceptualization: Supporting; Formal analysis: Supporting; Methodology: Supporting; Validation: Supporting; Writing – review & editing: Supporting)

Jinchuan Liu (Data curation: Supporting; Formal analysis: Supporting; Methodology: Supporting; Writing – review & editing: Supporting)

Tian Qin (Data curation: Supporting; Formal analysis: Supporting; Validation: Supporting; Writing – review & editing: Supporting)

Xiangqian Gu (Data curation: Supporting; Formal analysis: Supporting; Validation: Supporting; Writing – review & editing: Supporting)

Ji Wu (Formal analysis: Supporting; Methodology: Supporting; Writing – review & editing: Supporting)

Yi Zhang (Data curation: Supporting; Methodology: Supporting; Writing – review & editing: Supporting)

Honglin Wang (Conceptualization: Equal; Methodology: Equal; Project administration: Equal; Resources: Lead; Supervision: Equal; Writing – review & editing: Equal)

Yuanjia Tang (Conceptualization: Lead; Investigation: Equal; Methodology: Lead; Project administration: Lead; Resources: Equal; Supervision: Lead; Writing – review & editing: Lead)

Feng Xue, Professor (Conceptualization: Lead; Funding acquisition: Lead; Investigation: Lead; Methodology: Lead; Project administration: Lead; Resources: Lead; Supervision: Lead; Writing – review & editing: Lead)

Yimin Mao (Conceptualization: Equal; Methodology: Equal; Project administration: Equal; Supervision: Equal; Writing – review & editing: Supporting)

Qiang Xia (Funding acquisition: Equal; Project administration: Equal; Supervision: Equal; Writing – review & editing: Supporting)

Conflicts of interest

The authors disclose no conflicts.

Funding